Phase-field modeling of hydraulic fracture interaction with natural fractures

Eduarda M. Ferreira[1], Roque L. S. Pitangueira[1], Lapo Gori[1]

[1]*Structural Engineering Department, Federal University of Minas Gerais*
Av. Antonio Carlos, 6627, Pampulha, Belo Horizonte, 31270-901, Minas Gerais, Brazil
eduardaferreira@ufmg.br, roque@dees.ufmg.br, lapo@dees.ufmg.br

Abstract. The problem of hydraulic fracturing has been the subject of several studies in recent years, including different proposals for analytical, experimental, and numerical models. This interest is justified by the complexity of the problem and its great relevance, with applications in various areas including the industrial, energy and engineering sectors. Several applications deal with natural reservoirs which are usually characterized by the presence of inclusions, heterogeneities and natural fractures, the latter being the subject of this study. These pre-existing fractures affect the circulation of the pressurized fluid inserted into the reservoir, influencing the path of the hydraulic fracture. The interaction between hydraulic and natural fractures generates complex fracture propagation patterns involving arrest, cross and branch phenomena between the cracks. In this sense, an interesting approach to modeling hydraulic fracturing is the use of phase-field models (PFM). Through its variational approach, the PFM is able to automatically deal with any number of cracks without restricting their shapes or trajectories and the crack path is obtained directly as part of the solution to the energy minimization problem. Therefore, this paper proposes a study of the interaction between hydraulic fractures and different networks of pre-existing natural fractures using a PFM that considers the pressure load on the surface of the hydraulic fractures. Numerical examples are presented to illustrate different possible interactions between the cracks and to explore different initial crack scenarios. All simulations were performed using the INSANE (INteractive Structural ANalysis Environment) software.

Keywords: Phase-field modeling, Hydraulic fracture, Natural fracture network

1 Introduction

In hydraulic fracturing, the propagation of the fracture is directly related to the presence of the hydraulic pressure load inside the fracture. The study of this problem can result in complex models, taking into account the interactions between the deformed solid, the fluid flow and the fracturing propagation. Due to this complexity, most authors choose to propose simplifications in their models, which limit them to the intended application, but make the problem of hydraulic fracture more treatable. This fact led to the emergence of different approaches with varying applicability and limitation.

An interesting approach that has been extensively researched in the last decade in hydraulic fracturing modeling is the phase-field model (PFM). The PFM is related to the variational approach to brittle fracture, proposed by Francfort and Marigo [1] and overcome some computational fracture mechanics challenges due to its intrinsic characteristics such as automatic crack initiation, treating an arbitrary number of cracks without restricting their shapes or propagation directions and obtaining the fracture as part of the solution to an energy minimization problem.

In this sense, the PFM is a suitable model for studying hydraulic fracturing and its complex iterations with possible pre-existing natural fractures. According to Li et al. [2], a hydraulic fracture (HF) when interacting with natural fractures (NFs) can stop, branch, arrest or offset. These iterations affect the trajectory of the hydraulic fracture, making it essential to investigate them, especially in natural and geological materials, where the presence of faults, inclusions and interfaces is more common [3].

This paper aims to analyze possible interactions between HF and NFs considering variations in the properties of NFs and different scenarios of distribution of these pre-existing fractures within an elastic medium. The approach proposed by Bourdin et al. [4] is used to model the pressurized fractures. The model considers a constant pressure load in the fracture domain, which is taken into account by including an additional term in the total energy functional. All the implementation and numerical simulations were carried out in the INSANE (INteractive

Structural ANalysis Environment) software.

2 Phase-field modeling of hydraulic fracture

In the phase-field modeling for fracture, the fracture is represented from an additional field variable, the phase-field variable ϕ, which assumes unitary values along the crack, null values in intact regions of the solid and intermediate values between these two regions. Figure 1(a) illustrate the problem of diffuse fracture studied by the PFM, where $\mathcal{B}$ represents the broken part of the domain and $\partial\mathcal{B}$ is its boundary. The smooth transition between intact and damaged material in region $\mathcal{B}$ is governed by a material-associated parameter, called length scale l_0. In Fig. 1(a), Ω is the problem domain with external boundary $\partial\Omega$, consisting of a part where Dirichlet conditions are applied ($\partial\Omega_D$) and another part where Neumann conditions are applied ($\partial\Omega_N$). In the hydraulic fracturing problem, the crack surface is subjected to a pressure load, represented by p_f.

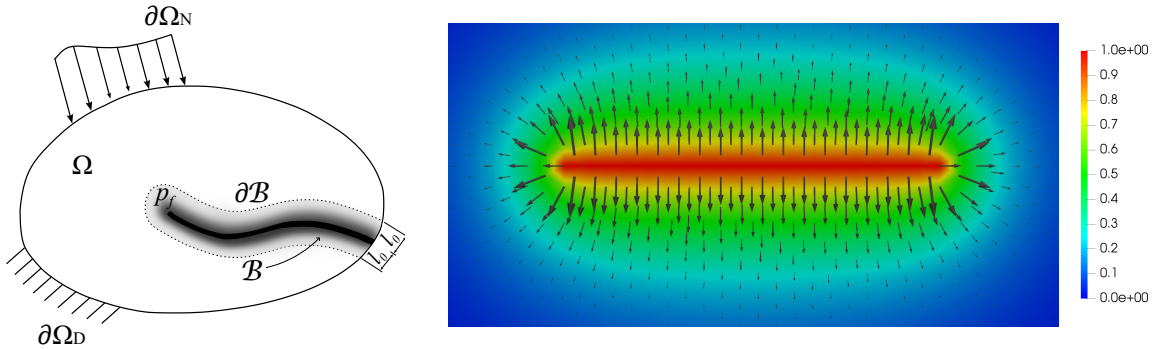

(a) (b)

Figure 1. Phase-field model: (a) A solid body with a phase-field crack with pressure load; (b) Negative phase-field gradient vector.

The PFM is based on the principles of energy minimization, in which the equilibrium state of an elastic solid body is reached by minimizing the potential energy of the system and the crack propagation occurs when the energy stored in the body exceeds the energy required for crack. The total energy functional for the fracture problem with pressure loading, that depends on the displacement field u and on the phase-field ϕ, can be written as:

$$E_t(u,\phi) = \int_\Omega \psi(\varepsilon(u),\phi)d\Omega + \int_\Omega G_c\gamma(\phi,\nabla\phi)d\Omega - \int_\Omega b\cdot u\, d\Omega - \int_{\partial\Omega_N} t\cdot u\, d\Omega_N + \int_\Omega p_f u\cdot\nabla\phi\, d\Omega, \quad (1)$$

where the integrals with body forces b and surface forces t represent external load potential energy, ψ is the strain energy density, ε is the linearized strain field $\varepsilon = (\nabla u + \nabla^T u)/2$, G_c is the critical fracture energy and γ is the crack surface density, that can be equated as follows:

$$\gamma(\phi,\nabla\phi) = \frac{1}{C_0}\left[\frac{1}{l_0}\alpha(\phi) + l_0|\nabla\phi|^2\right], \quad (2)$$

with $C_0 = 4\int_0^1 \alpha^{1/2}(\phi)d\phi$ and $\alpha(\phi)$ being the geometric crack function that defines how the phase-field distribution will occur along the degradation band.

In eq. (1), the last integral refers to the additional term added to the energy functional to account for the effects of the pressure load on the fracture surface. This is an approximation proposed by Bourdin et al. [4] where the surface force applied to the crack faces is translated into an appropriately scaled body force in the vicinity of the crack. According to this formulation, the hydraulic pressure load is closely related to the gradient of the phase-field variable. Figure 1(b) shows the negative phase-field gradient vector, which is responsible for indicating the direction of the pressure load.

The solution to the pressure driven fracture problem is obtained by minimizing eq. (1). The weak form of the problem is given by:

$$\begin{cases} \displaystyle\int_\Omega \sigma : \delta\varepsilon \, d\Omega = \int_\Omega (b - p_f \nabla\phi) \cdot \delta u \, d\Omega + \int_{\delta\Omega_N} t \cdot \delta u \, d\delta\Omega_N & \text{(3a)} \\ \displaystyle\int_\Omega \left[g'(\phi) \frac{\partial \psi}{\partial g} \delta\phi + G_c \delta\gamma + p_f u \cdot \nabla\delta\phi \right] d\Omega \geq 0, & \text{(3b)} \end{cases}$$

where $g(\phi)$ is the the energy degradation function and with crack surface density variation $\delta\gamma$ being defined by:

$$\delta\gamma = \frac{1}{C_0} \left[\frac{1}{l_0} \alpha'(\phi)\delta\phi + 2 l_0 \nabla\phi \cdot \nabla\delta\phi \right]. \tag{4}$$

To solve the phase-field problem presented, this work employed the staggered bound-constrained solver, proposed by Farrell and Maurini [5]. In this strategy, the solution of one of the variables is performed considering the other constant and the total energy functional minimization problem is treated as an optimization problem.

3 Interactions between hydraulic and natural fractures

The presence of natural fractures can significantly interfere with the trajectory of the hydraulic fracture, being responsible for the occurrence of complex phenomena such as crossing, bifurcation and off-setting between the fractures. According to Li et al. [2], some factors that can influence the behavior of the iteration between HF and NF are: the in-situ stress state, the fluid pressure, the fluid injection rate and the position and characteristics of NFs, such as their inclination and mechanical properties. Figure 2 shows the possible interactions between the hydraulic fracture and the natural fracture indicated by Lepillier et al. [6].

Yoshioka et al. [3] suggest that NFs can represent actually pre-existing fractures, flaws in the porous or elastic medium, or interfaces cemented with weaker or stronger materials. Thus, NFs can affect the trajectory of the HF in different ways depending on the case to be studied.

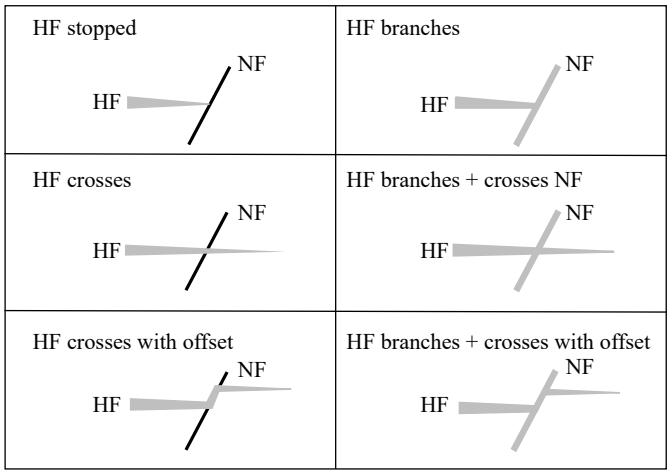

Figure 2. Interactions between the hydraulic fracture and the natural fracture. (adapted from [6])

4 Numerical examples

This section will present some numerical examples involving the propagation of hydraulic fractures in an elastic medium with the presence of pre-existing natural fractures. Some variations in the characteristics of the natural fractures are proposed as a way of exemplifying different types of possible HF-NF interactions. As pointed out by Li et al. [2], natural fractures are not always open. Therefore, only hydraulic fractures are represented as open regions contoured by the condition $\phi = 1$. Natural fractures are treated as regions of different toughness than the rest of the domain. The boundary conditions and increasing fluid pressure $p_f = 0.1\Delta t$ are maintained in all examples, where Δt is the analysis step. In addition, the quadratic functions $g(\phi)$ and $\alpha(\phi)$ proposed by Bourdin

et al. [7] and the constitutive model by Miehe et al. [8] are considered. A plane stress state and unit thickness are assumed in all models.

4.1 Hydraulic fracturing with a natural fracture

This example aims to evaluate the influence of the inclination and properties of the natural fracture on its interaction with a hydraulic fracture. The problem consists of a quadrilateral domain with a horizontal hydraulic fracture in its center and a natural fracture with same dimensions that can assume different initial inclinations. The dimensions and boundary conditions of the model are presented in Fig. 3(a). The analysis consists of 30 load steps and the dimensionless material parameters of the domain are: Young's modulus $E = 1.0$, Poisson's ration $\nu = 0.2$, fracture toughness $G_c = 1.0$, and length scale $l_0 = 0.044$. The mesh used in the analysis contains triangular elements with $h = 0.022$ near the initial fractures and $h = 0.4$ near the problem contour, in order to observe the relation $l_0/h \leq 2$ where the crack is expected to occur. A clip of the mesh is shown in Fig. 3(b).

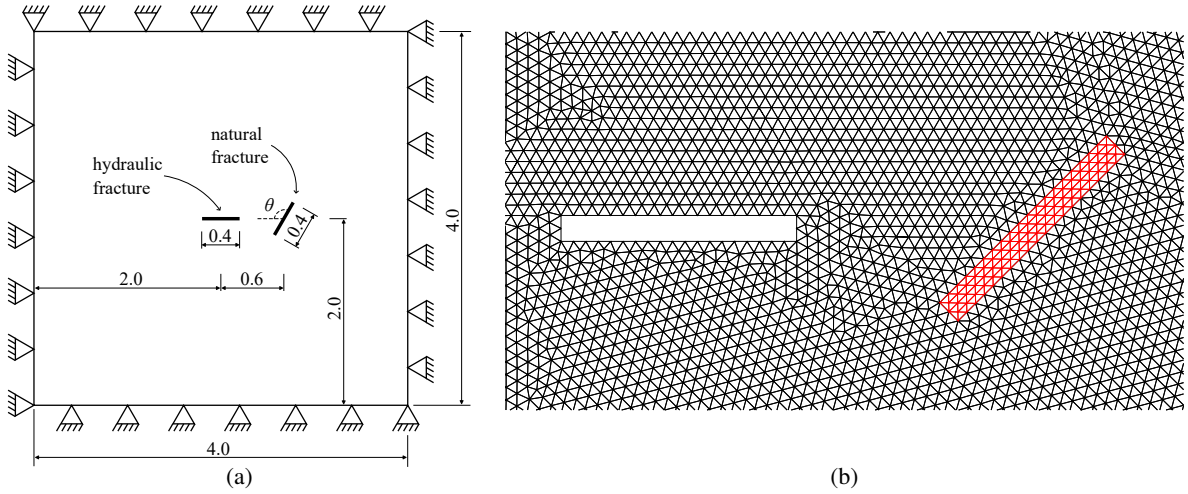

Figure 3. Hydraulic fracturing with a natural fracture: (a) Problem setting; (b) Detail of the T3 mesh. The HF is represented by the geometric discontinuity in the mesh and the NF is represented by the elements in red ($\theta = 45°$).

First, natural fractures with seven different inclinations are analyzed: $\theta = 0°$, $\theta = 15°$, $\theta = 30°$, $\theta = 45°$, $\theta = 60°$, $\theta = 75°$, and $\theta = 90°$. In all cases, the NF has the same material parameters as the rest of the domain, except for the fracture toughness, which is assigned 10% of the value of the domain, i.e. $G_c^{NF} = 0.1$. Figure 4 shows the phase-field contours obtained, where it is possible to see how the final crack pattern is affected by the inclination of the NF. For the angles $\theta = 0°, 15°, 30°, 45°$, the HF branches with the NF and they continue to propagate as a single crack, with a deviation from the initial trajectory depending on the approaching angle between HF and NF. For $\theta = 60°, 75°, 90°$ angles, after the branch between HF and NF occurs, the two ends of the NF begin to propagate, generating a pattern similar to a bifurcation, which becomes more noticeable as θ increases.

A second analysis of the same problem setting sought to evaluate the influence of the parameter G_c of the NF on its interaction with the HF. For this study, the initial inclinations of the NF $\theta = 0°, 30°, 60°, 90°$ and four variations of its critical fracture energy were considered: $G_c^{NF} = 0.1$, $G_c^{NF} = 0.5$, $G_c^{NF} = 1.0$ and $G_c^{NF} = 2.0$. The results obtained are presented in Fig. 5. It can be noticed that for $G_c^{NF} = 0.1$ the HF branches with the NF, regardless of the initial inclination of the NF. For $G_c^{NF} = 0.5$, the HF and NF branch only for small NF inclinations ($\theta = 0°, 30°$), while the HF crosses the NF for larger NF inclinations ($\theta = 60°, 90°$). When $G_c^{NF} = 1.0$, i.e. the same as the rest of the domain, the HF always crosses the NF. For $G_c^{NF} = 2.0$, the HF deviates from the NF, following a trajectory above it, when $\theta = 0°, 30°$ and the HF crosses the NF when $\theta = 60°, 90°$.

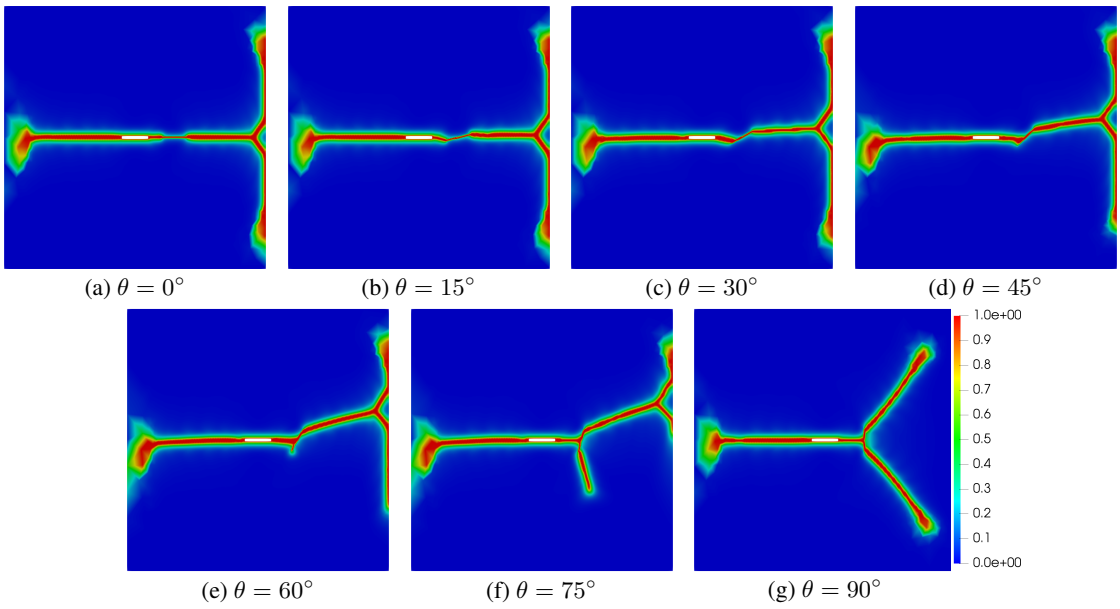

(a) $\theta = 0^\circ$ (b) $\theta = 15^\circ$ (c) $\theta = 30^\circ$ (d) $\theta = 45^\circ$

(e) $\theta = 60^\circ$ (f) $\theta = 75^\circ$ (g) $\theta = 90^\circ$

Figure 4. Phase-field contour plot: hydraulic fracturing interacting with natural fracture of different angles θ.

4.2 Multiple natural fractures test

This second example was designed to investigate a more complex network containing a greater number of NFs with different initial positions and inclinations. The initial fracture pattern and dimensions of the problem were inspired by the square plate with 10 random cracks test presented by Wu et al. [9]. The boundary conditions and distribution of the initial fractures across the domain are provided in Fig. 6. The dimensionless material parameters are: Young's modulus $E = 1.0$, Poisson's ration $\nu = 0.3$, fracture toughness $G_c = 1.0$, natural fracture toughness $G_c^{NF} = 0.1$, and length scale $l_0 = 0.02$. The entire domain was discretized using a mesh of triangular elements of characteristic size $h = 0.01$.

Figure 7 shows the crack path at different steps of the analysis. The HF begins its propagation approximately symmetrically to the right and left sides of the domain. The right-hand tip encounters the NF6 with which it branches. From this connection, the lower tip propagates towards the contour of the model and the upper tip crosses with offset the NF4. Meanwhile, the left-hand tip of the HF crosses with offset the NF5 and then bifurcates as it approaches the contour. The other NFs did not interact with the HF during the analysis. The complex pattern of the final crack highlights the importance of considering the possible cracks and interfaces present in the medium when modeling the hydraulic fracturing problem.

5 Conclusions

The purpose of this work was to study the possible iterations between hydraulic and natural fractures using the phase-field model for fractures with internal pressure proposed by Bourdin et al. [4]. The first numerical example sought to show the influence on the variation of the inclination and fracture toughness of the natural fracture on its interaction with a horizontal hydraulic fracture. It was possible to notice that the approaching angle between the hydraulic fracture and the natural fracture was relevant in defining whether branching, crossing or crossing with offset would occur. The ratio of the critical fracture energy of the natural fracture and the medium G_c^{NF}/G_c^{DOMAIN} is also an important parameter to be investigated, since for lower values of G_c^{NF} the branching phenomenon is more common, while for higher values of G_c^{NF}, the hydraulic fracture tends to cross the natural fractures. Different combinations of natural fracture inclination and G_c^{NF}/G_c^{DOMAIN} ratio produced different interaction and propagation behaviors, making it important to correctly consider both. The second numerical example explored a situation that could be applied to a real case study, representing a geological material in which there are several natural fractures distributed randomly, for example. The natural fractures were responsible for the deviation of the hydraulic fracture from its initial path, and it was important to take them into account when modeling the problem in order to correctly predict the path of the hydraulic fracture. It can be concluded

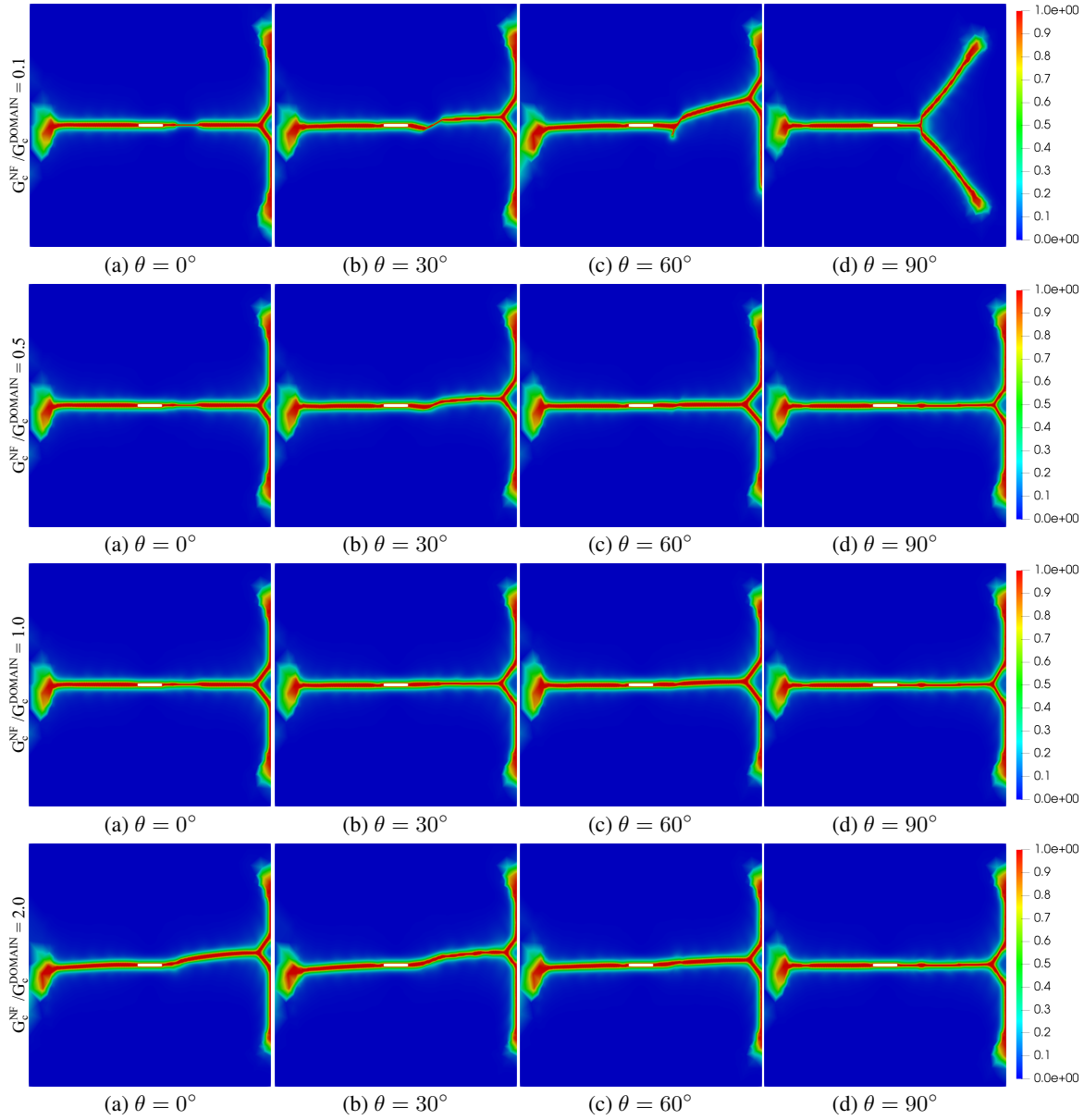

Figure 5. Phase-field contour plot: hydraulic fracturing interacting with natural fracture of different angles θ and different critical fracture energy G_c^{NF}.

that the model employed was able to successfully represent different possible iterations between hydraulic and natural fractures and that it is a relevant study for understanding the behavior of hydraulic fracturing and its correct trajectory in different scenarios.

Acknowledgements. The authors gratefully acknowledge the support from the Brazilian research agencies CAPES (*Coordenação de Aperfeiçoamento de Pessoal de Nível Superior*), FAPEMIG (*Fundação de Amparo à Pesquisa do Estado de Minas Gerais*; Grant PPM-00747-18) and CNPq (Conselho Nacional de Desenvolvimento Científico e Tecnológico; Grant 316240/2021-4).

Authorship statement. The authors hereby confirm that they are the sole liable persons responsible for the authorship of this work, and that all material that has been herein included as part of the present paper is either the property (and authorship) of the authors, or has the permission of the owners to be included here.

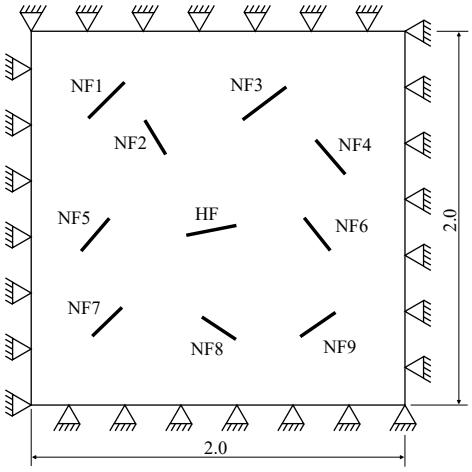

Figure 6. Problem setting: Multiple natural fractures test.

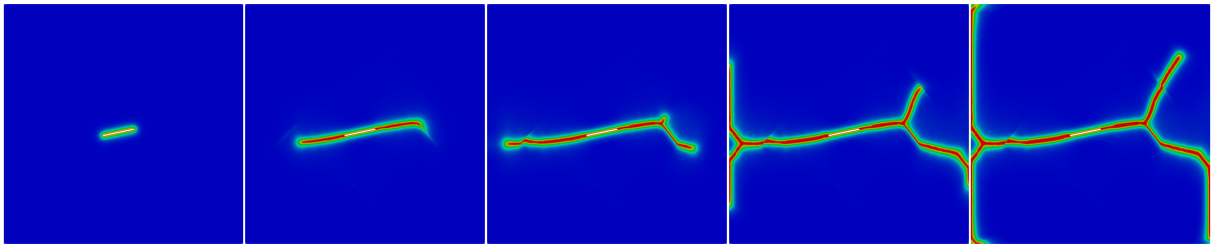

(a) (b) (c) (d) (e)

Figure 7. Phase-field contour plot - Multiple natural fractures: (a) Step 10; (b) Step 27; (c) Step 30; (d) Step 38; (e) Step 50.

References

[1] G. Francfort and J.-J. Marigo. Revisiting brittle fracture as an energy minimization problem. *Journal of the Mechanics and Physics of Solids*, vol. 46, n. 8, pp. 1319–1342, 1998.

[2] X. Li, H. Hofmann, K. Yoshioka, Y. Luo, and Y. Liang. Phase-field modelling of interactions between hydraulic fractures and natural fractures. *Rock Mechanics and Rock Engineering*, vol. 55, pp. 6227–6247, 2022.

[3] K. Yoshioka, M. Mollaali, and O. Kolditz. Variational phase-field fracture modeling with interfaces. *Computer Methods in Applied Mechanics and Engineering*, vol. 384, 2021.

[4] B. Bourdin, C. Chukwudozie, and K. Yoshioka. A variational approach to the numerical simulation of hydraulic fracturing. *Proceedings of the 2012 SPE Annual Technical Conference and Exhibition*, vol. SPE 146951, 2012.

[5] P. Farrell and C. Maurini. Linear and nonlinear solvers for variational phase-field models of brittle fracture. *International Journal for Numerical Methods in Engineering*, vol. 109, n. 5, pp. 648–667, 2017.

[6] B. Lepillier, K. Yoshioka, F. Parisio, R. Bakker, and D. Bruhn. Variational phase-field modeling of hydraulic fracture interaction with natural fractures and application to enhanced geothermal systems. *Journal of Geophysical Research: Solid Earth*, vol. 125, n. 7, 2020.

[7] B. Bourdin, G. Francfort, and J. J. Marigo. Numerical experiments in revisited brittle fracture. *Journal of the Mechanics and Physics of Solids*, vol. 48, pp. 797–826, 2000.

[8] C. Miehe, F. Welschinger, and M. Hofacker. Thermodynamically consistent phase-field models of fracture: Variational principles and multi-field FE implementations. *International Journal for Numerical Methods in Engineering*, vol. 83, pp. 1273–1311, 2010.

[9] J.-Y. Wu, V. P. Nguyen, C. T. Nguyen, D. Sutula, S. Sinaie, and S. P. Bordas. Chapter one - phase-field modeling of fracture. In S. P. Bordas and D. S. Balint, eds, *Advances in Applied Mechanics*, volume 53, pp. 1–183. Elsevier, 2020.